

# EVALUATING THE INFLUENCE OF CONTINUOUS FLAP SETTINGS ON THE APPROACH PERFORMANCE OF AN AIRLINER USING FLIGHT SIMULATION

P. Stukenborg, R. Luckner, Technische Universität Berlin, Institut für Luft- und Raumfahrt,  
Marchstr. 12, 10587 Berlin, Germany

## Abstract

This paper describes a method to investigate the benefits of a new high-lift system with continuously moving slats and flaps. The approach is evaluated, where a typical airliner decelerates during descent. The slat/flap setting is configured stepwise after the maximum allowable speed of the next slat/flap configuration is reached. Thus, most of the time the aircraft does not fly in its aerodynamic optimal configuration. The new system automatically adapts the slat/flap setting based on the airspeed and aircraft mass and enables the aircraft to fly with the aerodynamic optimal configuration. The performance is analysed using a flight simulation of a typical mid-range airliner and under variation of the conditions for a standard approach procedure. The assessment tool CoFA (Continuous Flap Assessment), developed in the project Con.Move, is capable of analysing performance benefits of continuous slat/flap settings. This paper describes and demonstrates the method by showing the influences of continuously moving slats and flaps on flight path, duration of the approach and fuel consumption for five different control laws for the extension of the slats/flaps using the tool CoFA. It gives an overview of the simulation environment and the developed functions of the tool, describes the approach procedure, and shows the resulting flight path for the different control laws.

## Keywords

continuous flap settings, approach, flight mechanical model, flight simulation, high-lift system

## Nomenclature

$\alpha$	angle of attack
$C_D$	drag coefficient
$C_L$	lift coefficient
$c_{c/eq/n/p}$	config value (continuous/equivalent/next/previous)
$\delta_{fl,sl}$	deflection of flap or slat
$g$	standard gravitational acceleration
$\gamma$	flight path angle
$H_{AGL}$	altitude above ground level
$m$	mass
$\rho$	density
$S$	wing area
$S$	horizontal distance from runway threshold
$V_{act}$	actual airspeed
$V_{app}$	approach airspeed
$V_{CAS}$	calibrated airspeed
$V_{dec,p/n}$	decision speed previous/next
$V_{IAS}$	indicated airspeed
$V_{FE,std}$	speed laws (config. change), highest flap extent speed
$V_{LS}$	speed laws (configuration change), lowest selectable
$V_{Drag,m.}$	speed laws (config. change), minimal drag
$V_{GD}$	speed laws (config. change), green dot
$V_{P_{aero,m.}}$	speed laws (config. change), min. aero. power loss

## Abbreviations

AGL	above ground level
ATC	air traffic control
CoFA	tool for continuous flap assessment
FCU	flight control unit
ILS	instrument landing system
MLM	maximum landing mass
MSL	mean sea level

## 1 INTRODUCTION

In the project Con.Move, TU Berlin investigates the use of continuous flap settings for the high-lift system of a mid-range aircraft. Until now, most airliners deflect the flaps and slats in fixed steps. The slats/flaps are extended after the maximal allowable speed for the next higher slat/flap setting is undershoot. During aircraft design, typically four or five fixed settings are defined based on the needed performance for take-off and landing. Commonly the slats/flaps are fully extended to achieve a very large lift coefficient for landing (called config 5 in this paper). The resulting significant increase of induced drag is accepted for landing. For take-off, where drag should be minimal, three or more settings between the clean configuration (config 0) and the landing configuration allow compromises between large lift coefficients and minimum increase of drag coefficient. The Airbus A350 uses flap deflections ( $< 4^\circ$ ) for drag reduction during cruise flight in order to vary the wing's camber [7]. The Boeing 787 features a similar variable camber function for cruise [1]. The McDonnell Douglas MD-11 has a system called Dial-A-Flap that allows the selection of intermediate flap positions degree-wise for take-off [6].

Each standard slat/flap setting corresponds to a certain airspeed for an optimal glide ratio. Since the aircraft accelerates during departure and decelerates during approach, the flap settings are not flown at their aerodynamic optimum most of the time. This can be improved by a high-lift system, which continuously adjusts the slat/flap setting in accordance to the current airspeed. During approach air traffic control (ATC) requires a target airspeed to control separation of arriving aircraft. Especially during head wind conditions the capacity of airports is reduced, when the traditional distance-based separations are applied. This unwanted reduction is addressed by time-based separation (TBS) approaches, newly introduced to e.g. London-Heathrow [2]. To maintain a high capacity of airports the arrival time during different wind conditions is an important factor to analyse.

The aim of the project Con.Move is the development of an assessment method for new high-lift systems. The Continuous

Flaps Assessment tool CoFA assesses the benefits of continuous flap settings for the approach procedure.

## 2 SIMULATION ENVIRONMENT

The tool CoFA analyses the impact of continuously moving slats and flaps on aircraft performance data. It consists of four main functions that are realised as software modules. Figure 1 shows a block diagram of the tool structure. The module "Inputs" defines all input parameters of the simulation, such as atmospheric and aircraft conditions. The simulation environment includes a high-fidelity flight mechanical simulation. The flight simulation runs online, thus the cockpit inputs are generated in a real cockpit environment. For the implementation of the continuous flap setting function, the pilot inputs for the slat/flap lever are replaced by the submodule for automatic continuous slat/flap movements. The outputs of the simulation environment are used for the assessment of continuous slat/flap settings.

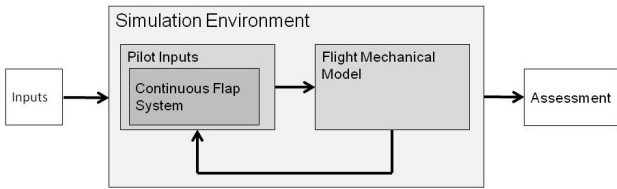


Figure 1: Block diagram of the CoFA tool structure.

### 2.1 Flight Mechanical Model

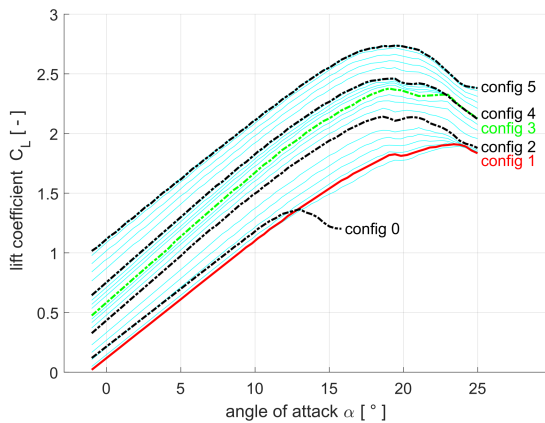


Figure 2: Lift polar for standard slat/flap settings in bold and interpolated values for continuous settings.

The flight simulation is based on an existing flight mechanical model of a conventional mid-range airliner. It is a standard non-linear, six degree-of-freedom model, which exists at TU Berlin and which is part of other projects and tools (e.g. [4] and [5]). It will not be described here in detail. Only the modifications of the aerodynamic model are explained, that are necessary to describe the effects of continuous slat/flap motion (cf. [8]). Figure 2 shows the lift coefficient  $C_L$  versus the angle of attack  $\alpha$  for different settings. The standard settings are marked in bold. As all settings between these standard settings shall be selectable, the intermediate aerodynamic data need to be

determined. As no data for the continuous settings are available yet, the aerodynamic values for the intermediate settings are interpolated between the existing values. Figure 2 shows in light blue the interpolated values. The interpolation is based on the deflection of slats and flaps.

To calculate the interpolated lift curves the slat and flap deflections are weighted and converted to an equivalent configuration value  $c_{eq}$

$$(1) \quad c_{eq} = \frac{\delta_{sl} + 5\delta_{fl}}{\delta_{sl,max} + 5\delta_{fl,max}},$$

with the deflection angle of the slats  $\delta_{sl}$ , the deflection angle of the flaps  $\delta_{fl}$  and normalized with the maximum deflection of both of them. The factors in Eq. 1 are chosen taking into account the influence of the deflection on the lift curve shown in Fig. 2. The flap deflection is weighted higher than the slat deflection angle, to reflect the higher influence of the flap deflection on the lift curve. The absolute values of the deflections are summarized in Tab. 1.

Table 1: Absolute slat and flap deflection for all configurations in degrees.

	config 1	config 2	config 3	config 4	config 5
slats	18	18	22	22	27
flaps	0	10	15	20	35

Figure 3 shows the equivalent values  $c_{eq}$  for the five different standard configurations *config* and the linear interpolation between them. Figure 4 shows the stepwise change of slat and flap settings as comparison to the continuous value (cf. Fig. 3).

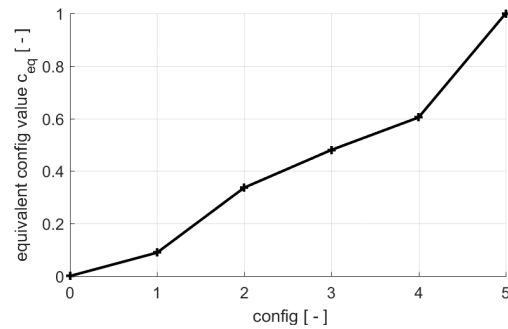


Figure 3: Equivalent configuration values as a function of normalized slat and flap deflections.

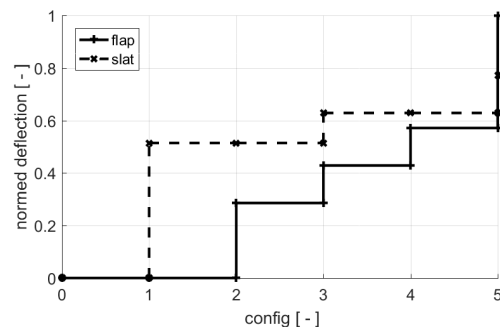


Figure 4: Normed configuration value (max. flap deflection) for standard stepwise slat/flap settings.

The value  $c_{eq}$  is then used to interpolate the values of lift and drag coefficients.

## 2.2 Slat/Flap Control Laws

To investigate the influence of different lift and drag coefficients the slat/flap movement is studied with five different control laws. The interpolation of aerodynamic data also depends on the chosen movement law. The five laws represent different control strategies:

- Law 0: highest possible flap extend speed, standard stepwise  $V_{FE,std}$ ,
- Law 1: speed of minimum drag coefficient  $V_{Drag,min}$ ,
- Law 2: lowest selectable speed  $V_{LS}$ ,
- Law 3: green dot speed (best glide ratio)  $V_{GD}$ , and
- Law 4: speed of minimal aerodynamic power loss  $V_{Paero,min}$ .

They ensure that the configuration fits to the airspeed. A state machine chooses between the laws. The effect of the control laws on the lift and drag coefficients when the indicated airspeed  $V_{IAS}$  is decreased is shown in Fig. 5. During the deceleration process, the slat and flap deflections change according to the chosen law, weight and actual airspeed. All laws start bottom right hand side of Fig. 5. The figure also shows that the aircraft has to decelerate longer to reach the speed of minimum drag coefficient and lowest selectable (Law 1 and 2), thus the slat/flap movement starts later than for the other laws. For each control law different decision speeds exist, one for each standard slat/flap configuration. The decision speeds are based on the aerodynamics of the standard slat/flap settings, which are exactly known. For law 0 (standard stepwise) config 2 is not selectable by the pilot during approach, therefore in Fig. 5 the configuration is skipped for the standard stepwise slat/flap setting.

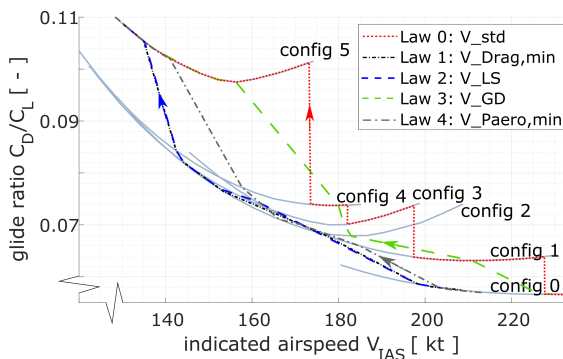


Figure 5: Glide polars for the standard slat/flap settings using the five different movement laws.

## 2.3 Decision Speed Calculation

The glide polar is mass dependent. Thus, the decision speeds need to be calculated with respect to mass.

$$(2) \quad V = \sqrt{\frac{2 \cdot mg \cdot \cos(\gamma)}{\rho \cdot S \cdot C_L}} \sim \sqrt{m}$$

with the flight path angle  $\gamma$ , the density  $\rho$  and the wing area  $S$ . For four different masses that represent the full mass range of the standard mid-range airliner, the decision speeds have

been determined for all five standard configuration settings of slats and flaps. Figure 6 shows that a linear approximation fits this relationship very well in the relevant mass range. This is true for all laws. Therefore, a linear interpolation between the decision speeds for every standard slat/flap setting depending on mass is implemented for all control laws (cf. [8]).

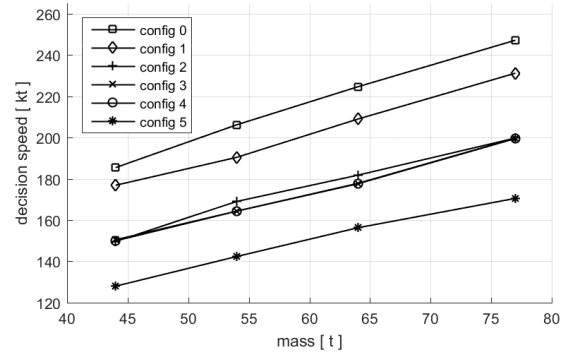


Figure 6: Decision speed for all standard configurations as a function of mass.

The decision speeds are calculated with the actual mass. The continuous configuration command value  $c_{c,cmd}$  depends on the actual configuration  $c_c$  and actual airspeed  $V_{IAS}$ . It is linear interpolated between the continuous config values shown in Fig. 3 and the actual velocity compared to the decision values calculated before using

$$(3) \quad c_{c,cmd} = c_p + \frac{c_n - c_p}{V_{dec,n} - V_{dec,p}} \cdot (V_{act} - V_{dec,p}),$$

where  $V_{act}$  is the current velocity and the indices  $n$  and  $p$  refer to the next and previous configuration. The continuous config value  $c_{c,cmd}$  as implemented to the simulation environment is described by the linear approximation of the neighbouring equivalent values of the standard configurations  $c_n$  and  $c_p$ , and the respective decision speeds  $V_{dec,n}$  and  $V_{dec,p}$ .

When the aircraft decelerates so fast that the movement of the flaps cannot follow, the indices  $n$  and  $p$  may not refer to direct neighbour configurations (e.g. config 1 and 3). This results in a higher gradient and therefore an enforcement of the deflection movement. The slat/flap setting config 2 with standard settings is not chosen by the pilot and only set during departure. As the aerodynamics for this setting are known, it is used for the linearisation of the aerodynamics between config 1 and config 3. The continuous value calculated with Eq. 3 is used as a command value. The output of the simulation is the effective configuration value, which is rate limited. Figure 7 shows the influence of the rate limitation on the command value  $c_{c,cmd}$ . The calculated  $c_{c,cmd}$  is based on the actual airspeed without system limitations. The continuous command value feeds the slat/flap system simulation. If the rate limitation of the implemented actuators is reached, the resulting configuration value  $c_c$  changes slower than the command value  $c_{c,cmd}$ .

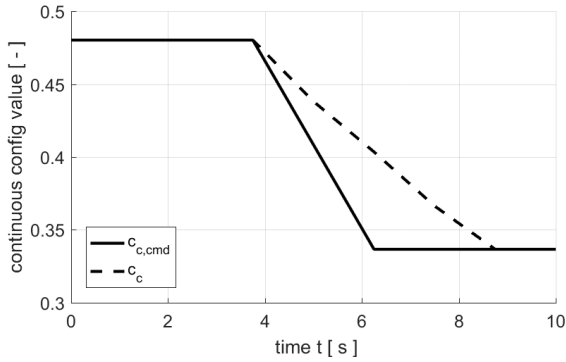


Figure 7: Comparison of commanded continuous config value  $c_{c,cmd}$  and the rate-limited result  $c_c$ .

The  $c_{c,cmd}$  is based on the following three conditions. First, it is checked if the speed is below the slat/flap maximal speed. If not, no deflection change is initiated. Second, the actual airspeed is compared to the decision speeds of the five standard configurations. Third, the actual configuration is checked to distinguish between the gradients with which the slat/flap position changes. The output of the system is the continuous config value  $c_{c,cmd}$  calculated with Eq. 3.

### 3 TOOL DEMONSTRATION

The functions and the capabilities of the CoFA tool are demonstrated by using the control laws for continuous slat/flap settings for a typical mid-range airliner.

#### 3.1 Demonstration Example

To analyse and assess the influence of continuous slat/flap settings, different flight parameters shall be considered. The main indicators for the assessment are:

- thrust setting,
- airspeed,
- flight time, and
- fuel consumption.

The approach procedure is a standard ILS approach to Tegel airport (EDDT 26R). Figure 8 shows the flight path and indicates the main decision criteria to change between different speeds and descent rates.

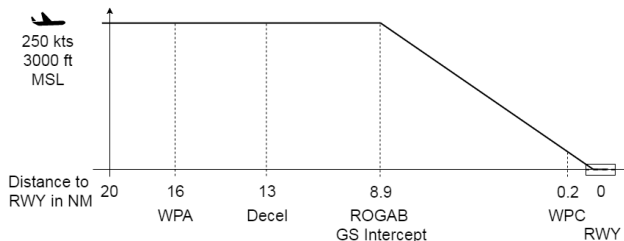


Figure 8: Approach procedure and criteria, according to the standard ILS approach [3].

The flight simulation starts 20 NM before the runway at 3000 ft MSL and with 250 kts calibrated airspeed. The aircraft is trimmed to this configuration for horizontal flight. The data assessment starts at waypoint WPA which is 16 NM from the

runway. The autopilot is in speed and altitude mode and the localizer is captured. The deceleration starts 13 NM from the runway and is initiated by entering the approach speed  $V_{app}$  to the FCU panel. The active movement law schedules the slat and flap setting according to the speed. Glide slope intercept is at ROGAB ( $\approx 8.9$  NM from the runway). The landing gear is extended after config 3 is fully deployed. If deceleration is too low, the landing gear is extended earlier to support the deceleration process. When the aircraft descends below  $H_{AGL} = 2500$  ft and is still in clean configuration, the landing gear is extended to enforce the deceleration process. The latest extension of the landing gear is when the aircraft descends below  $H_{AGL} = 1500$  ft. This procedure is the same for every simulation run, thus the resulting flight paths are similar. Energy balance and fuel consumption can be compared and it is possible to investigate the influence of the different control laws, on those parameters.

mass	config	wind	airspeed	flap rate
MLM	0	000/00	250 kt	1 °/s

Table 2: Summary of the initial data, where MLM is the maximum landing mass.

### 3.2 Results and Discussion

The assessment of continuous flap and slat settings is demonstrated by varying the five control laws for slat and flap retraction and the following three parameters:

- wind direction,
- constant wind vs. turbulence, and
- possible ATC speed schedule.

#### 3.2.1 Influence of Control Laws

The first evaluation compares the influence of the five different slat/flap movement control laws. It uses the initial data noted in Tab. 2. The results are analysed based on flight trajectory, configuration schedule, airspeed during the approach procedure and fuel consumption.

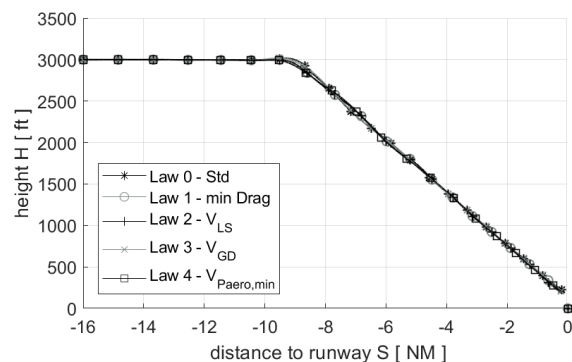


Figure 9: Flight paths depending on the slat/flap control law.

Figure 9 shows the flight paths for all laws. As the procedure and ILS path are given, the flight path is identical for all flap/slat movement laws. But airspeed varies for each flap/slat movement law (cf. Fig. 10). The extension of the flaps is speed dependent and the deceleration of the aircraft depends on the flap extension, therefore the airspeed is influenced by the different flap movement laws. Law 0 and law 3 act similar as

well as law 1 and law 2. The airspeed development for law 4 lies between the results of all other laws. The airspeed result correlates with the continuous config value shown in Fig. 11.

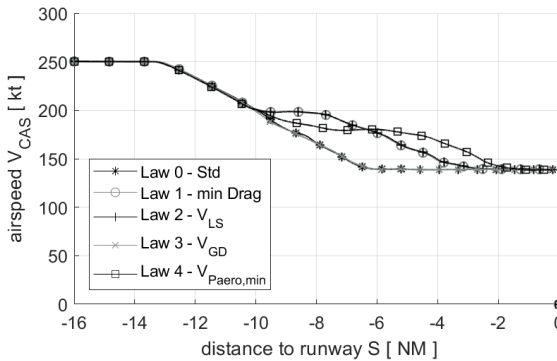


Figure 10: Airspeed depending on the slat/flap control law.

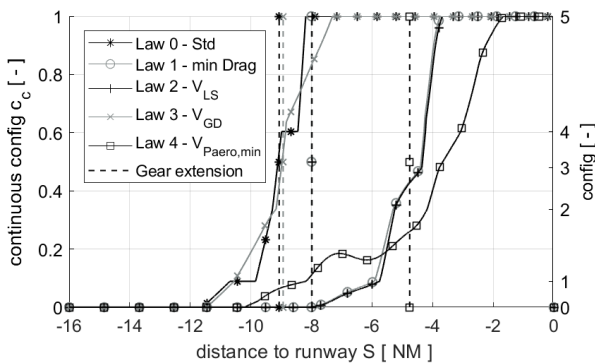


Figure 11: Continuous config value versus the distance between aircraft and runway depending on the slat/flap control law.

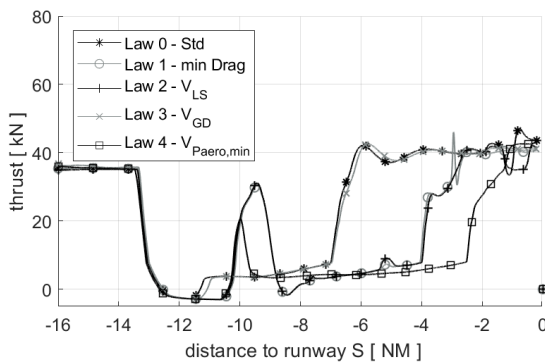


Figure 12: Thrust setting versus the distance from runway depending on the slat/flap control law.

For law 0 (standard flap movement) and law 3 (green dot speed) the flap movement is initiated earlier than for all other laws. The first slat/flap movement starts in a distance of 11 NM from the runway. For law 3 the full landing configuration is reached 7 NM from the runway. Thus, the extension takes more time than for law 0, which is fully extended during 3 NM (both have a similar airspeed, cf. Fig. 10). The earlier extension of the flaps results in higher drag and therefore in airspeed reduction. As a result more engine thrust is needed to maintain

the glide path (cf. Fig. 12). Law 1 and law 2 need additional thrust approximately 10 NM from the runway, because the slats extend so slowly, that the auto thrust reacts to avoid airspeed falling below the lowest selectable speeds  $V_{LS}$ . The higher thrust setting results in a higher fuel consumption and the earlier deceleration in a longer duration of the approach.

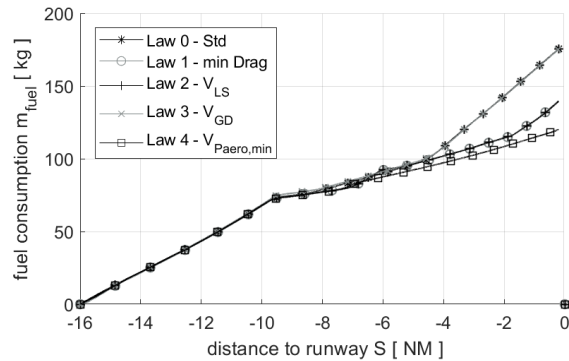


Figure 13: Total fuel consumption for the approach versus the distance from runway depending on the slat/flap control law.

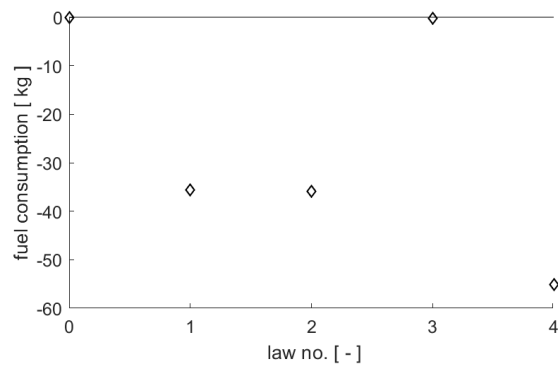


Figure 14: Difference in fuel consumption for all continuous configuration laws compared to the standard slat/flap setting.

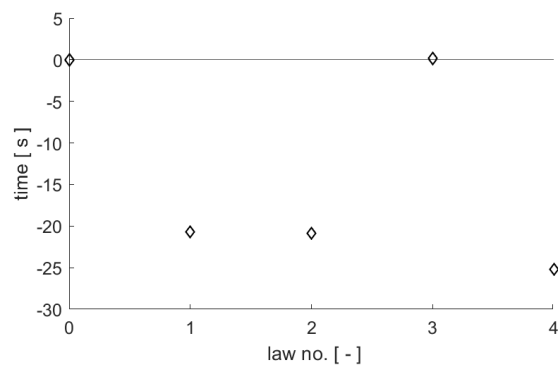


Figure 15: Difference in duration of the approach for all continuous configuration laws compared to the standard slat/flap setting.

Figure 13 shows the total fuel consumption depending on the distance to runway. As the thrust setting for law 0 and law 3 rises around 6 NM from the threshold (cf. Fig. 12), also the fuel consumption rises. In total 175 kg of fuel are burned between waypoint A and waypoint C. Whereas with law 4 only

120 kg of fuel are burned, which is more than 30% less. Figure 14 compares the absolute difference of fuel consumption between standard configuration and each continuous configuration law. Additionally, Fig. 15 shows the time needed for the approach compared for each continuous configuration law to the standard slat/flap setting.

The laws 1 and 2 (minimal drag coefficient and lowest selectable speed) act similar, as the decision speeds for these laws are nearly the same. Both reduce the fuel consumption significantly as well as the needed time for arrival. The results seem promising, but they are achieved by a delayed deceleration which is only possible with an earlier extension of the gear (before any flap movement is initiated). Furthermore, the decision speeds are so close to the minimal allowable speeds that the auto thrust increases the thrust setting to avoid that the speed undershoots the minimal allowable speed. This reaction is not favourable. The results for law 3 (best glide ratio) are similar to those of the standard setting. The results for law 4 (minimal aerodynamic power loss) are promising, as the fuel consumption is significantly reduced in comparison to the laws 1 and 2. In addition, the time of arrival can be reduced. With law 4 the aircraft arrives 5 s earlier and uses 20 kg less fuel than laws 1 and 2.

### 3.2.2 Influence of Constant Wind

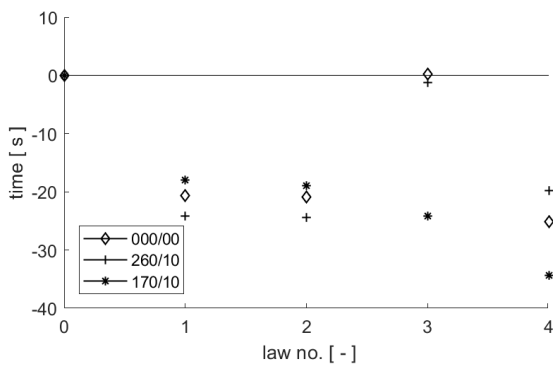


Figure 16: Difference in approach duration depending on the control law compared to the standard slat/flap setting for different wind conditions.

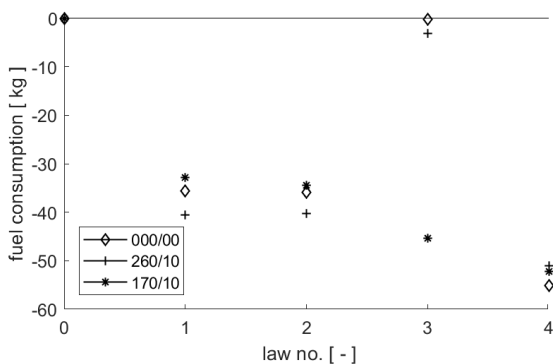


Figure 17: Difference in fuel consumption depending on the control law compared to the standard slat/flap setting for different wind conditions.

The arrival time is influenced by wind conditions. Especially, a

headwind component during approach reduces airport capacity, if the traditional distance-based separations are used. To maintain the capacity time-based separations are introduced. The time needed for the approach is therefore an important factor to assess the continuous flap system. The influence of crosswind and headwind are analysed and compared to the results without wind that are explained in Subsec. 3.2.1. As the approach is to runway 26, the headwind comes from 260° and the cross wind comes from 170°. Wind velocity is 10 kt in both cases. Figure 16 shows the time needed for the approach in comparison to the standard slat/flap setting for all continuous control laws. Besides law 3 (green dot speed), all continuous control laws reduce the needed arrival time. The approach with standard slat/flap settings takes 317 s. A reduction of 25 s equates approximately 8%. The shortest approach duration (35 s less than standard) is achieved with law 4 (minimal aerodynamic power loss). Accordingly the fuel consumption is even more reduced in head wind conditions (cf. Fig. 17). The maximal fuel reduction with a continuous control law is above 50 kg for one approach. In cross wind conditions (170° with 10 kt) the reduction is about five kilograms less, but still the fuel consumption can be significantly reduced comparing standard slat/flap settings with continuous slat/flap settings.

### 3.2.3 Influence of Turbulence

The calculated continuous configuration value is airspeed dependent. Every turbulence acts on the calculated value. To prevent flap movement caused by turbulence, the airspeed value that is used by the control law is filtered.

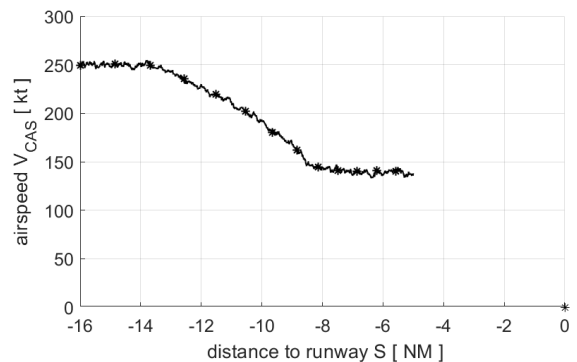


Figure 18: Airspeed for an approach under turbulent conditions.

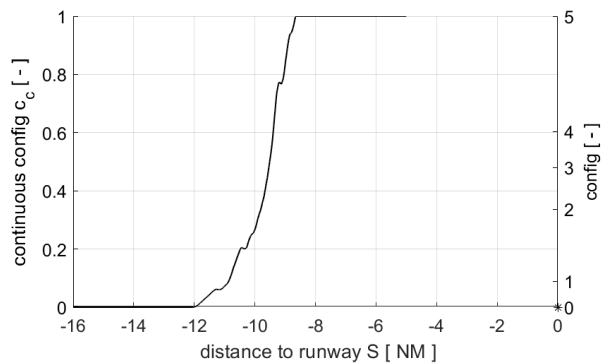


Figure 19: Continuous configuration value for turbulent conditions.

Figure 18 shows the measured airspeed value for an approach flown until the flaps are fully extended. Figure 19 shows the corresponding continuous configuration values. The turbulence is damped and retraction of the flaps is only initiated if the speed trend is positive. In future investigations safety aspects shall be analysed for automatic retraction during an approach scenario.

### 3.2.4 ATC Speed Schedule

During traffic peak times, approaching aircraft get speed targets from ATC to maintain slot times of the airport. The slat/flap setting is airspeed dependent and the influence of a fixed speed schedule shall be investigated. The approach is initiated with an airspeed of 250 kt like the standard configuration (cf. Tab. 2). At the deceleration point (Decel) the speed is not reduced to approach speed  $V_{app}$ , but to 190 kt to maintain a higher airspeed. At ROGAB the airspeed command is further reduced to 170 kt. At 1500 ft the commanded speed reduces to approach speed, so the approach can be stabilized in 1000 ft. The speed command is selected at the FCU panel. Figure 20 shows the airspeed for all control laws. Still the deceleration differs between the different control laws. For standard stepwise flap settings the deceleration is greater than for all other laws. Thus, the airspeed is the lowest during the deceleration process. The lower airspeed results in the longest duration of the approach (cf. Fig. 23). Compared to the results with continuous deceleration discussed in Subsec. 3.2.1 the differences in airspeed decrease. Figure 21 shows that higher airspeeds result in a shorter approach duration and lower thrust level compared to a continuous deceleration (cf. Fig. 12).

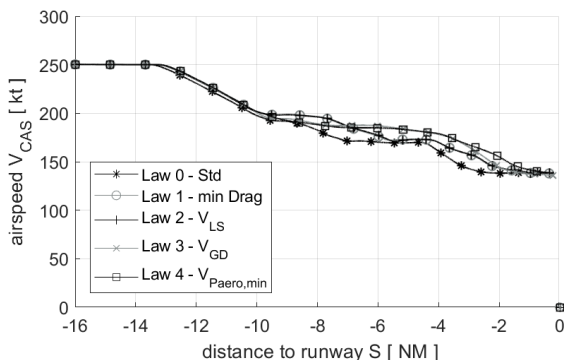


Figure 20: Airspeed versus the runway distance for all control laws.

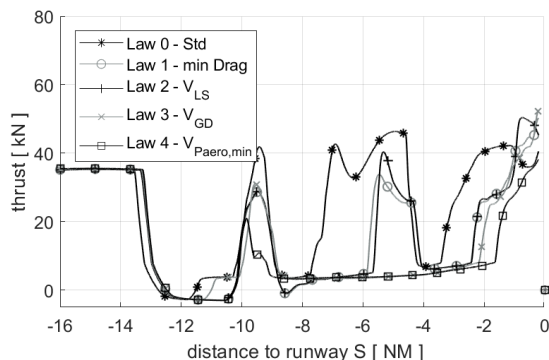


Figure 21: Thrust level versus the runway distance for all control laws.

Figure 22 and Fig. 23 show that the total duration difference between an approach with continuous flap control laws and the standard stepwise setting (law 0) decreases in case of an ATC speed schedule. But the fuel consumption difference is the same or even higher. The fuel consumption can be reduced up to 59 kg. The reduction is 5 kg more compared to the results discussed in Subsec. 3.2.1. Therefore, the main influence for fuel consumption is not the duration of the approach. When the approach duration is nearly the same the fuel consumption is significantly lower for an approach with continuous flap settings, than for the standard stepwise flap setting approach.

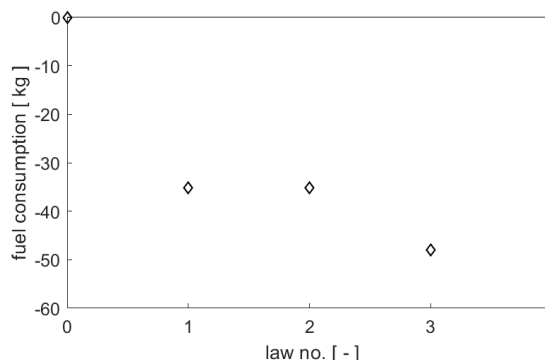


Figure 22: Fuel consumption for each continuous control law compared to the standard flap movement.

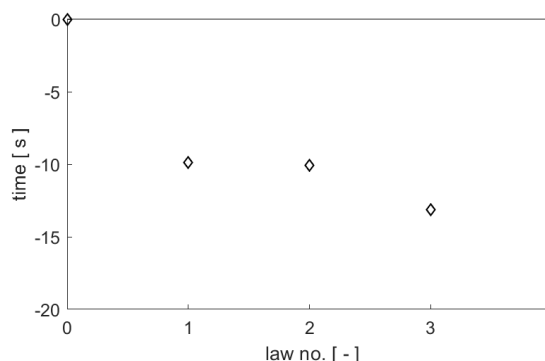


Figure 23: Duration of the approach for each continuous control law compared to the standard flap movement.

## 4 CONCLUSION

The focus of this paper is the development and demonstration of a method for the assessment of continuous flap control laws. The results that the tool CoFA computes are plausible. The assessment shows, that CoFA provides the expected information on the key performance indicators. Thus, the tool can be used to analyse the influence of other high-lift characteristics in further studies.

The benefits of a continuous control law for slats and flaps are relevant. The fuel consumption was reduced by 59 kg on the last 16 NM of the approach, which is more than 30% less compared to an approach with standard slat/flap settings. The control laws can cope with turbulence and no unwanted retraction during the approach phase was observed. Additionally, during headwind conditions the performance is better. An ATC speed

schedule for a faster approach reduces the total fuel consumption, as well as the relative fuel consumption using the continuous control laws. The simulation runs showed that the control laws based on lowest selectable speed and minimal drag coefficient are too close to the minimum airspeed restrictions. It is not possible to further reduce airspeed, when the auto thrust is active, because of the lowest selectable speed protection. The existing protection systems shall not be compromised by the new system of continuous flap settings. The results of this project Con.Move shall be an incremental product development, which is capable of being integrated to the current air traffic systems. Therefore, and because of the lowest total fuel consumption law 4 based on the minimal aerodynamic power loss is most promising. This result is consistent with an earlier study concerning take-off performance with continuous control laws for slats and flaps [8].

#### Acknowledgement

The work presented in this paper was funded by the German Federal Ministry for Economic Affairs and Energy (BMWi) due to resolution of the German Federal Parliament within the scope of the LuFo V/2 compound project CON.MOVE and TU Berlin's subproject AM-Move (grant number 20A1505D). The authors gratefully acknowledge this support.

#### REFERENCES

- [1] Boeing, ed. *Advanced Fly-by-wire - Variable Camber*. <https://www.boeing.com/commercial/787/by-design/#/advanced-fly-by-wire> visited: 10.10.2018. 2011.
- [2] Paul Haskin. *Explaining Time Based Separation at Heathrow*. Ed. by NATS. <https://nats.aero/blog/2014/02/explaining-time-based-separation-heathrow/> visited: 24.08.2018. Feb. 27, 2014.
- [3] Jeppesen. *JeppView 3.7.5.0*. Englewood, Colorado, USA: Jeppesen, 2015.
- [4] Vikram Krishnamurthy, Alexander Hamann, and Robert Luckner. "Automatisierte Prozesskette zur flugmechanischen Bewertung von Parameteränderungen im Rahmen des modellbasierten Flugzeugvorentwurfs". In: (2015). presented at DLRK, URN: 101:1-201601222820.
- [5] Vikram Krishnamurthy and Robert Luckner. "Flight Mechanical Modelling considering Flexibility and Flight Control Functions in Preliminary Aircraft Design". In: (2017). presented at AIAA Modeling and Simulation Technologies Conference. DOI: 10.2514/6.2017-4332.
- [6] Airways Magazin, ed. *Countdown to Retirement: American Airlines Super 80s*. <https://airwaysmag.com/airchive/american-airlines-super-80s-2/> visited: 17.08.2018. Aug. 23, 2016.
- [7] Henning Strüber. "The Aerodynamic Design of the A350 XWB-900 High Lift System". In: (2014). [http://www.icas.org/ICAS\\_ARCHIVE/ICAS2014/data/papers/2014\\_0298\\_paper.pdf](http://www.icas.org/ICAS_ARCHIVE/ICAS2014/data/papers/2014_0298_paper.pdf), visited 07.08.2018.
- [8] Pia Stukenborg and Robert Luckner. "Evaluating the influence of continuous flap settings on the take-off performance of an airliner using flight simulation". In: *CEAS Aeronautical Journal* (June 13, 2018). ISSN: 1869-5590. DOI: 10.1007/s13272-018-0315-2.